

MESO-SCALE MODELLING OF DAMAGE AND FAILURE OF CONCRETE

Andrey P Jivkov¹, Jiaming Wang²

¹ Professor, The University of Manchester, Manchester, UK (andrey.jivkov@manchester.ac.uk)

² Dr, University of Sheffield, Sheffield, UK (jiaming.wang@sheffield.ac.uk)

ABSTRACT

The understanding of the mechanisms leading to damage initiation and fracture propagation in concrete has progressed substantially with the development of the meso-scale models and their analysis. Such models represent concrete as a three-phase composite, comprising mortar, aggregates, and the interfaces between them, referred to as the interfacial transition zones (ITZ). The construction of meso-scale models has followed two distinct paths: (1) synthetic generation using statistical data for aggregates volume fraction and size and shape distribution; and (2) using 3D images obtained by X-ray computed tomography. While the latter approach provides realistic geometry and connectivity of the different phases of concrete, the constructed meso-scale models have limited volumes, which may not be representative for analysis of damage and failure of concrete. The benefit of the former approach is that it allows to cover substantially larger volumes, potentially of the order of structural components. The aim of this work is to clarify the applicability of these approaches by investigating the macroscopic behaviour of concrete obtained with synthetic and image-based models. The models are prepared using previously established mechanical behaviours of the phases – elastic-brittle aggregates, elastic-plastic-damage behaviour of mortar, and cohesive elements for ITZ. Calibration of parameters for different phases and validation of models is performed by own experimental data. It is shown that both the image-based and the synthetic models yield results in good agreement with experiments under compressive and tensile loads. The simpler synthetic models are recommended in the derivation of stress-strain behaviour for analysis of engineering structures. Image-based models are suggested for analysis of coupled behaviour, e.g., mass transport with various loadings, including drying-wetting cycle and sustained loading, and high-temperature loading.

INTRODUCTION

Concrete is a quasi-brittle composite material, which dissipates mechanical energy by internal friction between constituents (sliding mode) and by generation of micro-cracks (opening mode). When concrete is considered as a homogeneous, isotropic continuum, which is typical for the engineering practice, these energy dissipation mechanisms are represented by standard modelling techniques (e.g., Lubliner et al., 1989; Lee and Fenves, 1998; Grassl and Jirásek, 2006; Badel et al., 2007; Wosatko et al., 2018). The sliding mode is akin to plasticity in metals, i.e., not associated with stiffness reduction, and therefore included in the description of concrete behaviour as plasticity. The opening mode is associated directly with stiffness reduction, and therefore included in the description of concrete behaviour as damage. However, the calibration of constitutive laws for concrete that involve plasticity and damage requires significant number of complex and costly experiments to capture the effects of different possible internal structures and stress states. Critically, the use of so calibrated constitutive laws for analysis of concrete behaviour will be strictly valid only when the plasticity and damage in a structural component are uniformly distributed. However, concrete is a composite material where plasticity, damage initiation, and crack propagation are associated

with localisation of energy dissipation by the concrete meso-structure (e.g., Wriggers and Moftah, 2006; Wang et al., 2016). This is a significant obstacle to the universal application of constitutive laws based on the assumption of homogeneous, isotropic material. Reliable integrity assessments of concrete structural components require in-depth analysis of localized crack initiation and propagation.

The meso-scale structure of concrete is formed by a mortar matrix, with possibly entrapped air voids, and large aggregates. In most meso-structural models the large aggregates are homogeneous, isotropic, elastic regions, i.e., possible damage or fracture of aggregates is neglected because their strength is higher than the concrete failure stress. This is adopted in the present work. On the other hand, the mortar is considered to include cement paste, sand, and fine aggregates, and represented by homogeneous, isotropic, inelastic regions. The mortar inelastic behaviour has been modelled by elastic-damage (e.g., Wang et al., 2016; Yilmaz and Molinari, 2017), elastic-plastic (e.g., Unger et al., 2011; Bonifaz et al., 2017), or elastic-plastic-damage (e.g., Chen et al., 2018; Wang et al., 2020) constitutive laws. The last approach is adopted in the present work.

Critical components of the meso-structure are the interfacial transition zones (ITZ) – thin layers of higher-porosity mortar coating the aggregates, with measured thickness between 10 and 50 μm (Xiao et al., 2013). They provide preferable locations for crack initiation and easier pathways for crack evolution due to their lower stiffness and strength compared with mortar. ITZ have been neglected in some works and the energy dissipation has been attributed only to mortar by an elastic-plastic (e.g., Bonifaz et al., 2017; Cui et al., 2018), or elastic-plastic-damage (e.g., Du et al., 2014) constitutive behaviour, but these approaches have been shown to lead to over-estimations of concrete strength, because the damage localisation due to ITZ is not captured (Wang et al., 2020). The incorporation of ITZ in meso-structural models of concrete has followed two paths. First, ITZ have been represented by layers of finite thickness surrounding aggregates, modelled with continuum finite elements with elastic-plastic-damage behaviour different from mortar (e.g., Du et al., 2014; Chen et al., 2018). In such case, due to the computational complexity, the ITZ thickness in the model is substantially larger than the physical one, but Maleki et al. (2020) have recently shown that such models can provide results with acceptable accuracy. Second, ITZ have been represented by layers of zero thickness between mortar and aggregates, modelled with cohesive elements (eg., Caballero et al, 2006; Wang et al., 2016). Wang et al. (2021) have compared different ITZ representations and found that the representation with zero-thickness cohesive elements balances the physical realism and the computational efficiency, while providing predictions for stress-strain behaviour and damage evolution in agreement with experimental data. This approach is adopted in the present work.

Concrete meso-structures have been constructed either using X-ray Computed Tomography (XCT) images, an approach referred to as the image-based modelling (e.g., Ren et al., 2015; Huang et al., 2015), or by in-silico generation using statistical data, an approach referred to as the parametric modelling (e.g., Wang et al., 2016; Zhang et al., 2018). While both approaches are increasingly used, little work has been done on comparing their performance in predicting measured macroscopic behaviour. Only recently, Wang et al. (2022) presented a systematic study of the predictions of the two approaches in comparison to experimental data for the stress-strain behaviour, damage initiation and propagation. This paper offers an overview of the experimental and modelling techniques used by Wang et al. (2022), together with in-depth discussion of the obtained results.

EXPERIMENTAL AND MODELLING BACKGROUND

Quasi-static experiments were performed with specimens made of mortar and of concrete. Uniaxial compression tests were conducted using cylindrical specimens of 100 mm diameter and 200 mm height. Uniaxial tension tests were conducted with dogbone specimens of 90 mm length and 25 mm thickness.

Results from tension and compression tests with mortar specimens were used to calibrate the elastic-plastic-damage constitutive law for mortar, which was then used as input to models of concrete specimens. Since mortar is a composite of cement, sand, and fine aggregates, it can be considered as concrete at a lower length-scale, whose constitutive behaviour is like the one used for concrete at the macroscopic scale. Appropriate description is provided by the concrete-damage-plasticity (CDP) model,

which captures the behaviour of concrete in tension and compression. The stress-strain response in compression is characterised by three stages: linear elastic behaviour, plastic behaviour with strain hardening prior to damage initiation, and strain softening with damage evolution. Mathematically, the stress-strain response in compression is described by (GB50010 2010):

$$\frac{\sigma_c}{\sigma_{cu}} = \begin{cases} \frac{E_0 \varepsilon_c}{\sigma_{cu}}, & \frac{\sigma_c}{\sigma_{c0}} \leq 0.4, \\ \alpha_a \frac{\varepsilon_c}{\varepsilon_{cu}} + (3 - 2\alpha_a) \left(\frac{\varepsilon_c}{\varepsilon_{cu}}\right)^2 + (\alpha_a - 2) \left(\frac{\varepsilon_c}{\varepsilon_{cu}}\right)^3, & \frac{\sigma_c}{\sigma_{c0}} \geq 0.4 \quad \& \quad \frac{\varepsilon_c}{\varepsilon_{cu}} \leq 1 \\ \frac{\frac{\varepsilon_c}{\varepsilon_{cu}}}{\alpha_d \left(\frac{\varepsilon_c}{\varepsilon_{cu}} - 1\right)^2 + \frac{\varepsilon_c}{\varepsilon_{cu}}}, & \frac{\varepsilon_c}{\varepsilon_{cu}} \geq 1, \end{cases} \quad (1)$$

where σ_c and ε_c are the current compressive stress and strain, σ_{c0} and ε_{c0} are the peak stress and strain, σ_{cu} and ε_{cu} are the stress and strain at damage initiation, α_a and α_d are parameters related to σ_{cu} . The stress-strain response in tension is characterised by two stages: linear elastic behaviour up to tensile peak stress, and post-peak softening behaviour described mathematically by (GB50010 2010)

$$\frac{\sigma_t}{\sigma_{t0}} = \frac{\frac{\varepsilon_t}{\varepsilon_{t0}}}{\alpha_t \left(\frac{\varepsilon_t}{\varepsilon_{t0}} - 1\right)^{1.7} + \frac{\varepsilon_t}{\varepsilon_{t0}}} \quad (2)$$

where σ_t and ε_t are the current tensile stress and strain, σ_{t0} and ε_{t0} are the peak stress and strain, and α_t is a coefficient related with σ_{t0} . Using the results from the compression and tension tests, the parameters involved in these equations were calibrated and given in Table 1.

Concrete specimens with 30% aggregate volume fraction were prepared with limestone aggregates with sieve size distribution between 6.3 and 10 mm. The same water-cement-sand mixes were the same as for the mortar specimens.

X-ray Computed Tomography (XCT) scanning of one cylindrical concrete specimen was carried out prior to mechanical test. 2D images were obtained and further reconstructed into 3D models for visualisation and phase segmentation. A core with diameter of 50 mm and height of 100 mm was cropped from the whole cylinder to reduce data processing time. Phase segmentation tool based on machine learning algorithms was used to identify concrete constituents. Detailed experimental design can be found in Wang et al. (2022). Figure 1 shows the segmented aggregate particles of the concrete model. This was used to create the image-based finite element model of a cylindrical specimen.

Synthetic models were constructed by random distribution of spherical aggregates with prescribed size distribution and voids with 1% volume content in the prescribed concrete volume. The detailed ‘take-and-place’ procedure used in the generation is described in Wang et al. (2016). Concrete models with 50 mm in diameter and 100 mm in height were generated to reduce computational cost. The same cylinders were adopted for uniaxial tension, because direct tension test, where dogbone samples were applied, was experimentally challenging for cylindrical specimens.

The volumes generated from XCT images or by parametrization were tessellated into voxels prior to generation of finite element mesh in image-based approach. Tetrahedral elements were used. Mesh sensitivity tests were carried out by Wang et al. (2021, 2022) and mesh with voxel size of 0.25 mm was adopted for parametric models. Zero-thickness cohesive elements (CE) were inserted at the interface between aggregate and mortar for the representation of ITZ via an in-house procedure. The behaviour of the cohesive elements was described by a traction-separation law, whose parameters are given in Table 1.

The finite element models of all specimens were loaded by prescribed displacements parallel to the cylinder axis. Zero displacements were set at one surface, while displacements at the other surface were applied by a rigid plate in compression and at surface nodes in tension. The energy dissipated by plasticity and damage was obtained for mortar and ITZ. One parametric realisation, i.e., one spatial distributions of

aggregates, was used for both tension and compression simulations, because the same stress-strain curves were obtained after testing different model realisations.

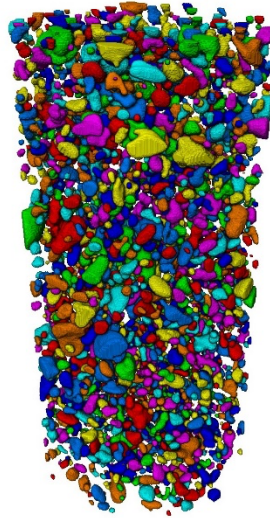


Figure 1. Segmented aggregate of concrete model from XCT images with 30% aggregate content.

Table 1. Parameters of the mechanical behaviour of concrete constituents

	Aggregate	Mortar	ITZ	
			Mode I	Mode II
Elastic moduli MPa	45	21.4	-	-
Density kg/m ³	2700	2200	2000	
Poisson's ratio	0.2			
Compressive strength MPa	-	49.7	-	-
Compressive critical strain	-	3.55E-3	-	-
Tensile strength MPa	-	3.7	-	-
Stiffness N/mm ³	-	-	1E5	
Critical strength MPa	-	-	3.5	10.5
Dissipation energy N/mm	-	-	0.03	0.09

RESULTS AND DISCUSSION

The mean peak stress and critical strain obtained by experiment and simulation are given in Table 2. Figures 2-5 show stress-strain curves, energy dissipation and damage patterns of concrete meso-structures with 30% aggregate volume fraction, which are generated from XCT scan and parametrically, under compression and tension. It is found that the compressive and tensile mechanical behaviour of parametric and XCT concrete models agree well with experimental results. Similar fracture pattern is observed for both models, the only substantial difference is the distribution of damage.

Table 2. Mean peak stress and critical strain of experiment, parametric model and XCT model

	Compression		Tension	
	Peak stress MPa	Critical strain	Peak stress MPa	Critical strain
Experiment	33.8	1.84E-3	3.68	1.96E-4
Parametric model	31.5	1.71E-3	3.63	1.76E-4
XCT model	35.0	1.94E-3	3.68	2.51E-4

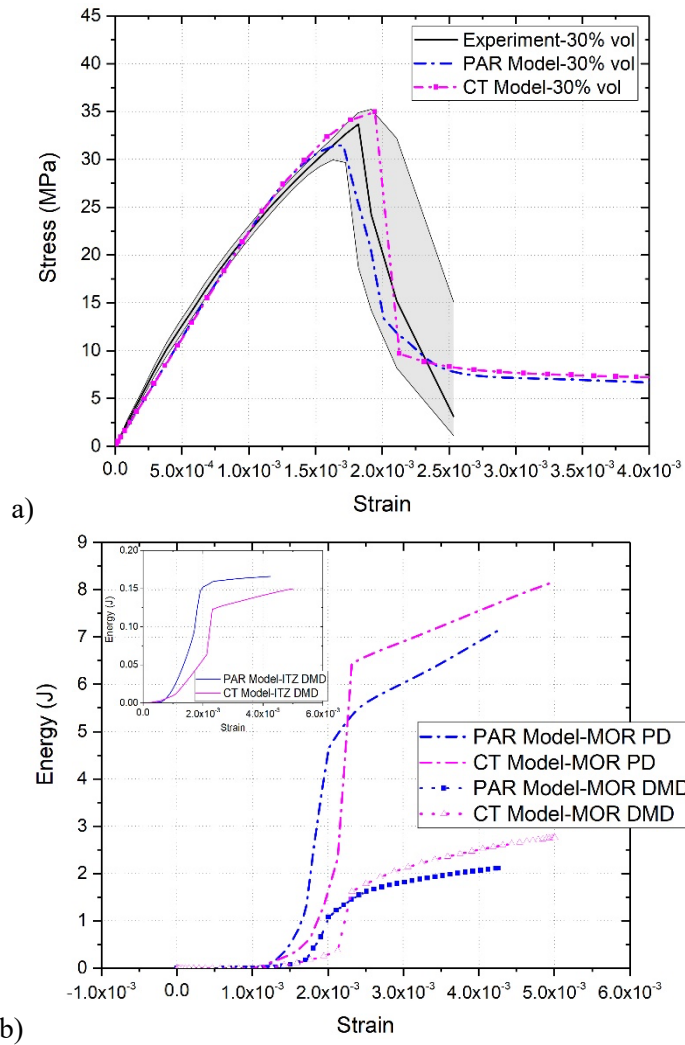


Figure 2. a) Stress-strain curves and b) energy output of parametric and XCT concrete models under compression

As illustrated in Fig. 2 (a), the peak strength and critical strain of both mesoscale models are in good agreement with experimental results. However, the peak strength predicted by the XCT model is 11% higher than that of the parametric model, which has been previously observed by Wang et al. (2016), and Xu and Chen (2016). Additionally, the critical strain of the XCT model is 13% higher. This can be explained by the irregular shapes of natural aggregates. The energy output of parametric and XCT model is shown in

Fig. 2 (b). The energy dissipated by plasticity (PD) of mortar and the energy dissipated by damage (DMD) of mortar and ITZ describe the inelastic mechanical behaviour of concrete meso-structure. The onset of plastic and damage dissipation of the XCT model is later than that of the parametric model. This is explained by the higher critical strain in the XCT model. The high energy dissipation rate of mortar and ITZ in XCT model is reflected in the rapid post-peak softening. Additionally, the XCT model shows larger energy dissipation via mortar plasticity and damage than the parametric model; extra energy was dissipated to attain the higher peak strength. Finally, the damage dissipation of ITZ in the XCT model is smaller than that in parametric model, because the total surface area of ITZ in the former is smaller.

Figure 3 compares the failure patterns of parametric and XCT models. Elements with damage value (SDEG) above 0.9 are considered fully failed. Even though the parametric and the XCT models have the same aggregate volume fraction, there are more aggregates in the later model, where denser packaging of aggregates is observed. The typical shear crack in Figure 3 is consistent with experimental observation in Wang et al. (2020). The failure patterns of both models are identical, but only the distribution of damage, especially for ITZ cohesive elements, is substantially different. The reason is that compared with the parametric model, the XCT model has more physically realistic aggregate size distribution and location.

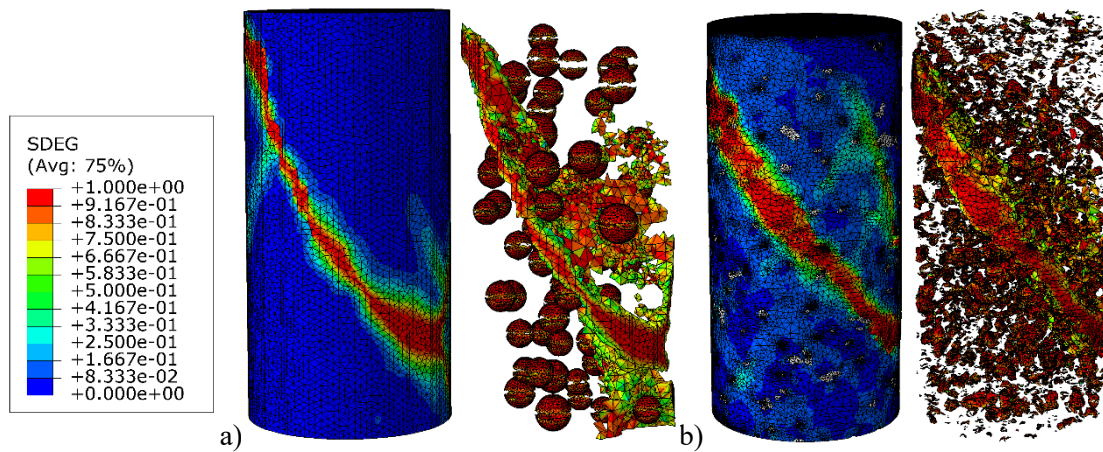


Figure 3. Crack patterns of a) parametric and b) XCT concrete models under compression

Figure 4 shows the stress-strain curves and energy output under tension. The peak strength and critical strain of the XCT model agree well with those of the parametric model, but the post-peak softening of the former is slower. This is because the tension of the XCT model leads to more energy dissipation. With the same plastic and damage dissipation of mortar, the ITZ damage dissipation of XCT model is ten times larger than that of parametric model. It can be explained by the fact that natural aggregates are more irregular, which leads to larger stress concentrations around sharp corners. Therefore, more damaged ITZ elements are observed in the XCT model, as seen in Fig. 5. One dominant crack develops in the middle of cylindrical specimen in both models.

Other than the substantial difference in the distribution of damage, the parametric and the XCT concrete models agree well with experimental observations. However, there are certain requirements for the construction of concrete meso-structures. For parametric models, self-developed code is needed to generate randomly distributed phase particles according to prescribed parameters. For XCT model, scanning of specimens is expensive and it is time-consuming to process CT images and segment phases.

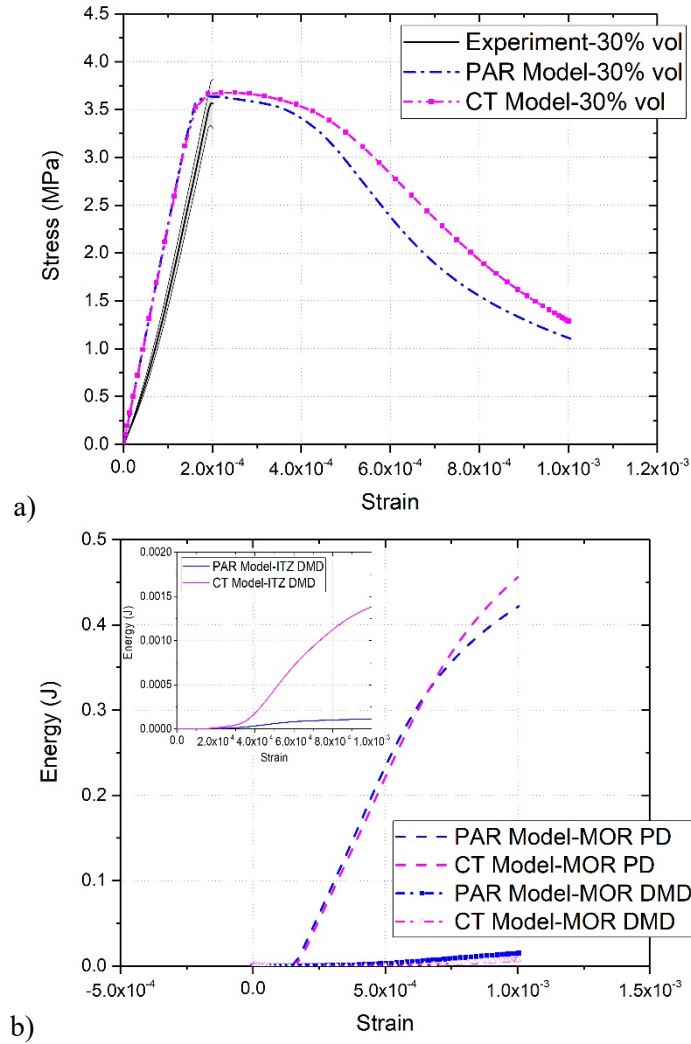


Figure 4. a) Stress-strain curves and b) energy output of parametric and XCT concrete models under tension

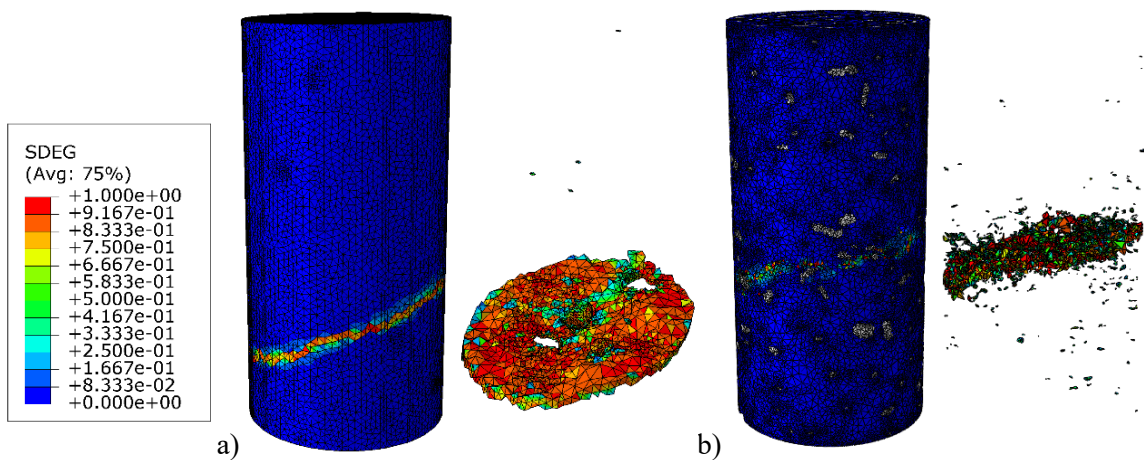


Figure 5. Crack patterns of a) parametric and b) XCT concrete models under tension

One advantage of parametric modelling is its ability to generate large volume meso-structures while preserving volume fraction and size distribution of aggregates. The volume of meso-structure is no longer limited by the XCT scanning requirement and can be used to investigate concrete size effects. When doing so, the ratio between aggregate size and component size should be consistent. This will clarify the notion of representative volume element for a given concrete component. In practice, parametric concrete models can be placed in the region where damage is expected to initiate and evolve. Therefore, this modelling approach can be used to assess the integrity of critical components in engineering structures.

XCT concrete models have the advantage in terms of their more realistic representation of the shape, size and spatial distribution of phase particles. Such models can be applied to verify hypotheses on the constitutive behaviour of different phases by performing in situ testing (i.e., scan the specimen during mechanical experiments). One limitation is the volume of the specimen that can be scanned, which does not guarantee the measured behaviour from the volume is representative for larger component. The present work demonstrates that good predictions of macro-scale stress-strain behaviour and failure process with both concrete models can be achieved by selecting constitutive behaviours with parameters calibrated via mortar tests or previous experience.

CONCLUSIONS

Image-based and parametric concrete meso-structures are used to simulate concrete mechanical behaviour under compression and tension. The effect of aggregate distribution is assessed via stress-strain data and damage patterns, while the mechanisms are explained via energy dissipation results. The main findings are summarised below:

- The practical and effective approach to simulate concrete under uniaxial compression, tension and potentially other loading conditions is to model concrete inelastic behaviour at meso-scale with plastic-damageable mortar and damageable ITZ represented by zero-thickness cohesive elements.
- The mechanical behaviour predicted by both image-based and parametric models agrees well with experimental results under compression and tension. The only difference between the two modelling approaches is the distribution of damage, which is explained by the difference in aggregate shapes.
- Image-based modelling is suggested for testing hypotheses for concrete constitutive behaviour, as well as for analysis of coupled behaviour, e.g., coupled mass transport and damage.
- Parametric modelling is suggested for analysing size effects and critical parts of engineering structures by engineering practitioners.

ACKNOWLEDGEMENTS

Wang acknowledges the support of Manchester X-ray Imaging Facility for using experimental facilities and IT Services for using Computational Shared Facility. Jivkov acknowledges gratefully the financial support of EPSRC via grant EP/N026136/1.

REFERENCES

- Badel, P., Godard, V., Leblond, J.B. (2007). "Application of some anisotropic damage model to the prediction of the failure of some complex industrial concrete structure." *International Journal of Solids and Structures*, 44, 5848–5874.
- Bonifaz, E.A., Baus, J., Lantsoght, E.O.L. (2017). "Modeling Concrete Material Structure: A Two-Phase Meso Finite Element Model." *Journal of Multiscale Modelling*, 8, 1750004.
- Caballero, A., López, C.M., Carol, I. (2006). "3D meso-structural analysis of concrete specimens under uniaxial tension." *Computer Methods in Applied Mechanics and Engineering*, 195, 7182–7195.

- Chen, H., Xu, B., Mo, Y.L., Zhou, T. (2018). "Behavior of meso-scale heterogeneous concrete under uniaxial tensile and compressive loadings." *Construction and Building Materials*, 178, 418–431.
- Cui, J., Hao, H., Shi, Y. (2018). "Study of concrete damage mechanism under hydrostatic pressure by numerical simulations". *Construction and Building Materials*, 160, 440–449.
- Du, X., Jin, L., Ma, G. (2014). "Numerical simulation of dynamic tensile-failure of concrete at meso-scale". *International Journal of Impact Engineering*, 66, 5–17.
- GB50010 (2010). "Chinese code for the design of reinforced concrete structures."
- Grassl, P., Jirásek, M. (2006). "Plastic model with non-local damage applied to concrete." *International Journal for Numerical and Analytical Methods in Geomechanics*, 30, 71–90.
- Huang, Y., Yang, Z., Ren, W., Liu, G., Zhang, C. (2015). "3D meso-scale fracture modelling and validation of concrete based on in-situ X-ray Computed Tomography images using damage plasticity model." *International Journal of Solids and Structures*, 67, 340–352.
- Lee, J., Fenves, G.L. (1998). "Plastic-Damage Model for Cyclic Loading of Concrete Structures." *Journal of Engineering Mechanics*, 124, 892–900.
- Lublinter, J., Oliver, J., Oller, S., Oñate, E. (1989). "A plastic-damage model for concrete." *International Journal of Solids and Structures*, 25, 299–326.
- Maleki, M., Rasoolan, I., Khajehdezfily, A., Jivkov A.P. (2020). "On the effect of ITZ thickness in meso-scale models of concrete." *Construction and Building Materials*, 258, 119639.
- Ren, W., Yang, Z., Sharma, R., Zhang, C., Withers, P.J. (2015). "Two-dimensional X-ray CT image based meso-scale fracture modelling of concrete." *Engineering Fracture Mechanics*, 133, 24–39.
- Unger, J., Eckardt, S., Könke, C. (2011). "A mesoscale model for concrete to simulate mechanical failure." *Computers and Concrete*, 8, 401–423.
- Wang, X., Zhang, M., Jivkov, A.P. (2016). "Computational technology for analysis of 3D meso-structure effects on damage and failure of concrete." *International Journal of Solids and Structures*, 80, 310–333.
- Wang, J., Jivkov, A.P., Li, Q.M., Engelberg, D.L. (2020). "Experimental and numerical investigation of mortar and ITZ parameters in meso-scale models of concrete." *Theoretical and Applied Fracture Mechanics*, 109, 102722.
- Wang, J., Li, X., Jivkov, A.P., Li, Q.M., Engelberg, D.L. (2021). "Interfacial transition zones in concrete meso-scale models – Balancing physical realism and computational efficiency." *Construction and Building Materials*, 293, 1–17.
- Wang, J.M., Jivkov, A.P., Engelberg, D.L., Li, Q.M. (2022). "Image-based vs parametric modelling of concrete meso-structures." *Materials*, 15, 704.
- Wosatko, A., Genikomsou, A., Pamin, J., Polak, M.A., Winnicki, A. (2018). "Examination of two regularized damage-plasticity models for concrete with regard to crack closing." *Engineering Fracture Mechanics*, 194, 190–211.
- Wriggers, P., Moftah, S.O. (2006). "Mesoscale models for concrete: Homogenisation and damage behaviour." *Finite Elements in Analysis and Design*, 42, 623–636.
- Xiao, J., Li, W., Corr, D.J., Shah, S.P. (2013). "Effects of interfacial transition zones on the stress-strain behavior of modeled recycled aggregate concrete." *Cement and Concrete Research*, 52, 82–99.
- Xu, Y., Chen, S. (2016). "A method for modeling the damage behavior of concrete with a three-phase mesostructure." *Construction and Building Materials*, 102, 26–38.
- Yilmaz, O., Molinari, J.F. (2017). "A mesoscale fracture model for concrete." *Cement and Concrete Research*, 97, 84–94.
- Zhang, J., Wang, Z., Yang, H., Wang, Z., Shu, X. (2018). "3D meso-scale modeling of reinforcement concrete with high volume fraction of randomly distributed aggregates." *Construction and Building Materials*, 164, 350–361.